https://doi.org/10.55343/CogSust.150

# Implementation of an optimised autonomous Arduino-based car

Dr. Clio Vossou
0000-0002-4665-7759
*Postdoctoral researcher, Vehicles Laboratory, National Technical University of Athens*
Athens, Greece
klvossou@mail.ntua.gr

Ioanna Konstantinou
*School of Mechanical Engineering, National Technical University of Athens*
Athens, Greece
joanna_constantinou@hotmail.com

Prof. Dimitrios Koulocheris
0000-0002-1379-5805
*Director of Vehicles Laboratory, National Technical University of Athens*
Athens, Greece
dbkoulva@mail.ntua.gr

**Abstract**

Autonomous vehicles can be a key feature to sustainable mobility since they promise optimised routes, more efficient fuel consumption, safer road transport, and the ability to alter the perception of driving. This paper describes the implementation of a low-cost, self-navigating Arduino-based model car. The model car utilises an Arduino Uno mainboard. Four DC motors with their corresponding wheels are embedded in the model car to ensure its movement. Furthermore, the model car has an ultrasonic sensor to detect and avoid obstacles. Moreover, the model car hosts an action camera to record its environment, and more features may be added later for artificial cognition. Its chassis is designed and optimised to accommodate all the electronic components and ensure movement. Different versions of the chassis were fabricated using 3D printing technology. The performance of the model car was assessed while navigating in three different scenarios, during which the effect of the speed of the model car and the efficiency of its ultrasonic sensor were evaluated. The paper concludes with the topology optimisation of the chassis of the model car to optimise the chassis compliance and consequently improve the navigation characteristics of the model car.

**Keywords**

autonomous vehicle, sustainability, Arduino, ultrasound sensor, topology optimisation

## 1. Introduction

Sustainability, in general, is a term associated with economy, environment and society (Ketter et al., 2023). Transportation is an important economic sector that is rapidly changing to keep up with policymakers' sustainability goals, especially in the EU (Bao et al., 2023; Buzási and Csete, 2015). This can be translated to efficient, zero-emission and safe vehicles in road transport. Enhancing vehicles with artificial cognition can optimise road transport sustainability.

According to the statistics for the greenhouse gas emissions in the European Union (Eurostat, 2024a), although between 2008 and 2023 the level of greenhouse gas (GHG) emissions from all economic activities decreased by approximately 25%, GHG emissions from transportation and storage activities remained almost unaltered. Furthermore, the number of registered passenger cars in the EU shows an increasing trend regarding passenger road transport. In 2023, the number of registered passenger cars reached almost 257 million, corresponding to an increase of 6.5% compared to 2018 (Eurostat, 2024b). As

https://doi.org/10.55343/CogSust.150

the number of passenger vehicles increases, and since most road accidents can be attributed to human error (Fathy et al., 2020), one can also expect an increase in road accidents. Hence, for the road transportation to become sustainable, it must be optimised in terms of environmental footprint and safety. At a system level, this could be achieved utilising artificial intelligence and cognitive info-communication (Orynycz, 2024). Electric, autonomous and connected road vehicles seem to enhance transportation sustainability and lead to the development of smart cities (Sheeba et al., 2021). Furthermore, the introduction of connected road vehicles with on-board sensors could lead to vehicle-level mobility decisions based on sustainability (Zöldy et al., 2022).

An autonomous road vehicle is a computer-controlled car with artificial cognition capabilities that can guide itself, familiarise itself with the surroundings, make decisions and fully operate without human interaction (Das et al., 2024). According to the Standard SAE J3016, driving automation has six levels, from Level 0 (No Driving Automation) to Level 5 (Full Driving Automation). While Level 1 (Driver Assistance) and Level 2 (Partial Driving Automation) have been successfully commercialised with features like lane-centring and Adaptive Cruise Control (ACC), achieving full driving automation (Level 5) remains the ultimate goal (SAE, 2018).

Autonomous cars' presence has also become imminent in public and industrial transport, including buses, taxis, trucks, and couriers. Especially for trucks, applications such as platooning seem to be gaining attention, although there are many challenges ahead before fully autonomous vehicles can become the main mode of transportation across the globe. Safety, ethics, psychology, and other profound fields will undoubtedly involve decision-making and policy formulation (Ciuciu et al., 2017).

In order to test concepts applied in cars that enhance transport sustainability, scale model cars can be developed. Due to their small size, scale model cars have a lower environmental footprint during production and operation stages than full-scale cars. The concepts of embedded automation systems can especially be tested on such scale models since they require lower financial effort and offer quick and reliable results, provided the model is properly built.

In the literature, several Arduino-based model cars exist with various capabilities. Some of these models are controlled via Bluetooth (Gandotra et al., 2016; Patil et al., 2022; Vijayalakshmi, 2019; Ankit et al., 2016; Chen et al., 2018; Simatupang et al., 2016; Tang et al., 2019; Yilmaz and Tariyan, 2019). The models designed by Ankit et al. (2016) and Yılmaz and Tariyan Özyer (2019) also have the capability of autonomous movement. The model cars described in Fathy et al. (2020), Claes et al. (2013) and Walke et al. (2022) host a camera for obstacle detection and incorporate more capabilities such as lane detection. However, the majority of the model vehicles utilise one or more (Ciuciu et al., 2017) ultrasonic sensors since they have emerged as a prevalent choice for measuring distances and facilitating obstacle avoidance in autonomous vehicles (Bhatia and Panchal, 2024). Table 1 summarises the capabilities of the Arduino-based model cars found in the literature:

Table 1. Arduino-based model cars in the literature

| | Control via Bluetooth | Autonomous movement | Camera | Ultrasonic sensor(s) |
|---|---|---|---|---|
| Ankit et al. (2016) | ✓ | ✓ | | ✓ |
| Bhatia and Panchal (2024) | | ✓ | | ✓ |
| Chen et al. (2018) | ✓ | | | ✓ |
| Ciuciu et al., 2017 | | ✓ | | ✓ |
| Claes et al. (2013) | | ✓ | ✓ | |
| Das et al. (2024) | | ✓ | | |
| Fathy et al. (2020) | | ✓ | ✓ | |
| Gandotra et al., (2016) | ✓ | | | |
| He et al. (2020) | | ✓ | | ✓ |
| Patil et al. (2022) | ✓ | | | ✓ |
| Rosen et al. (2014) | | ✓ | | ✓ |
| Simatupang et al., (2016) | ✓ | | | |
| Tang et al. (2019) | ✓ | ✓ | | ✓ |
| Vairavan et al. (2018) | | ✓ | | ✓ |
| Vijayalakshmi (2019) | ✓ | | | |
| Walke et al. (2022) | | ✓ | ✓ | |
| Yılmaz and Tariyan Özyer (2019) | ✓ | ✓ | | ✓ |

https://doi.org/10.55343/CogSust.150

It is worth mentioning that the typical design of model cars was described only in the works of Ankit et al. (2016), Yılmaz and Tariyan Özyer (2019) and Bhatia and Panchal (2024), and only a few results of their operation are described. Furthermore, little can be found concerning the performance evaluation of autonomous model cars or their use for developing real-scale autonomous vehicles. The use of scaled autonomous vehicles in the research and development of autonomous vehicles is illustrated by Ferencz and Zöldy (2021; 2022), who used scaled radio-controlled vehicle models to validate autonomous vehicles' movement in a roundabout.

The present paper presents the design and implementation of a self-navigating model car, and its performance in different navigation scenarios is evaluated. Additionally, the topology optimisation of its chassis in terms of mass is addressed. The paper begins with the description of the design methodology of the autonomous model car, which includes the selection of the electronic components, the mounting of hardware parts and the development of the necessary software code. Afterwards, the behaviour of the model car is monitored in different navigation manoeuvres, and the results are presented. Finally, the design of an optimised chassis is presented, considering the typical dimensions of normal-scale vehicles and the principles of topology optimisation.

## 2. Design methodology

In order to manufacture the proposed autonomous model car, the electronic components were first carefully selected. Then, a preliminary design of the chassis was created, taking into consideration the electronic components' shape and weight characteristics, and it was manufactured using 3D printing. Subsequently, the electronic components were mounted on the chassis. Finally, the software code was written and uploaded to the board.

### 2.1. Electronic components

As the central processing unit, the Arduino UNO R3 was selected. This board incorporates the ATmega328P 8-bit microcontroller. For the movement of the model car, the motor wheel kit was selected, consisting of 4 DC geared motors, four wheels and four holders. In order to control the DC geared motors, the Adafruit Motor/Stepper/Servo Shield for Arduino was utilised. This motor shield can control up to 4 DC motors or up to 2 stepper motors. For the model car to have an obstacle avoidance capability and be autonomous, the ultrasonic module distance sensor HC-SR04 was selected. The HC-SR04 is a proximity sensor with an input voltage of 5 VDC, which provides a 2 to 400 cm non-contact measurement function, and its ranging accuracy can reach up to 3 mm. Its measuring angle is 30°. Since the measuring angle of the HC-SR04 sensor is 30°, it was decided to mount it on the servomotor KS0194 with a rotation angle range of 180°. Finally, two 9 V rechargeable Li-ion batteries were used for the model car's power supply.

### 2.2. Chassis design and manufacturing

For the preliminary design of the chassis, the dimensions of the electronic components were taken into consideration, and an effort was made to reduce the chassis weight by removing material from areas which would not host any components. This led to the design (Design1) presented in Figure 1.

https://doi.org/10.55343/CogSust.150

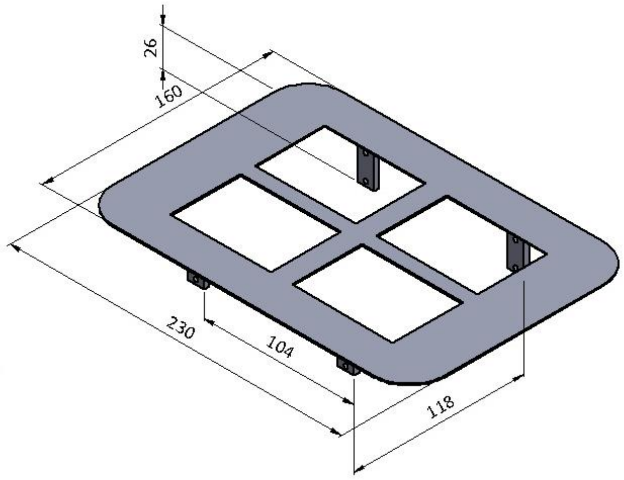


Figure 1. Chassis – preliminary design (Design 1)

The chassis was designed in Solidworks® and manufactured using fused deposition modelling in an Ultimaker S5 3D printer. The Ultimaker's Polylactic Acid (PLA) was selected as chassis material. The chassis is symmetric along the longitudinal (left–right) and the lateral (front–rear) axes. The outer dimensions of the chassis are 230 × 160 mm, with a wheelbase of 104 mm and a track width of 118 mm. Figure 2 presents the preliminary implementation of the autonomous model car.

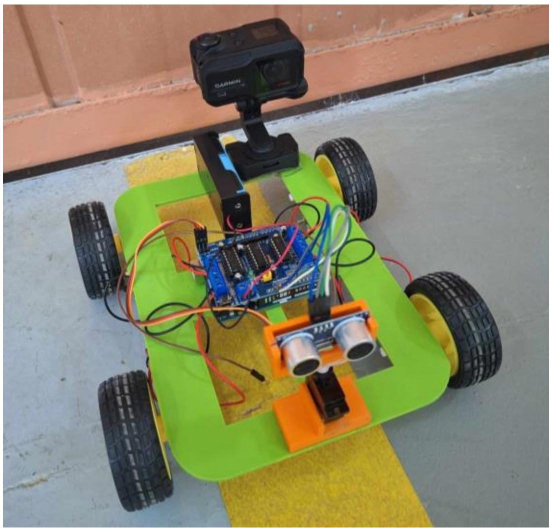


Figure 2. Preliminary implementation of the autonomous model car (Design 1)

The wheels' motors are mounted on the chassis. A DC motor controls each wheel without suspension and has a camber angle 0°. All the wheels are in contact with the ground and non-slipping conditions are hypothesised (Luu et al., 2019).

In Figure 2, the Garmin Virb action camera, used to monitor the movement of the model car, is visible at the rear of the model car. Furthermore, the placement of the battery pack can be observed. Additionally, the positioning of the ultrasonic distance sensor is crucial, as it correlates with the performance of the model car in obstacle detection and avoidance. Therefore, a special mounting can be observed. During the operation of this preliminary implementation, unwanted movement of the wheels around the vertical axis (Z-axis) was observed. Also, the influence of the non-symmetric placement of the action camera was observed. Therefore, the chassis was redesigned to ensure that the movement around the Z-axis of the four DC motors is restricted and that the battery pack can be hosted horizontally, lowering the centre of mass of the model car, improving its performance. Figure 3 presents the improved design (Design 2) of the chassis.

https://doi.org/10.55343/CogSust.150

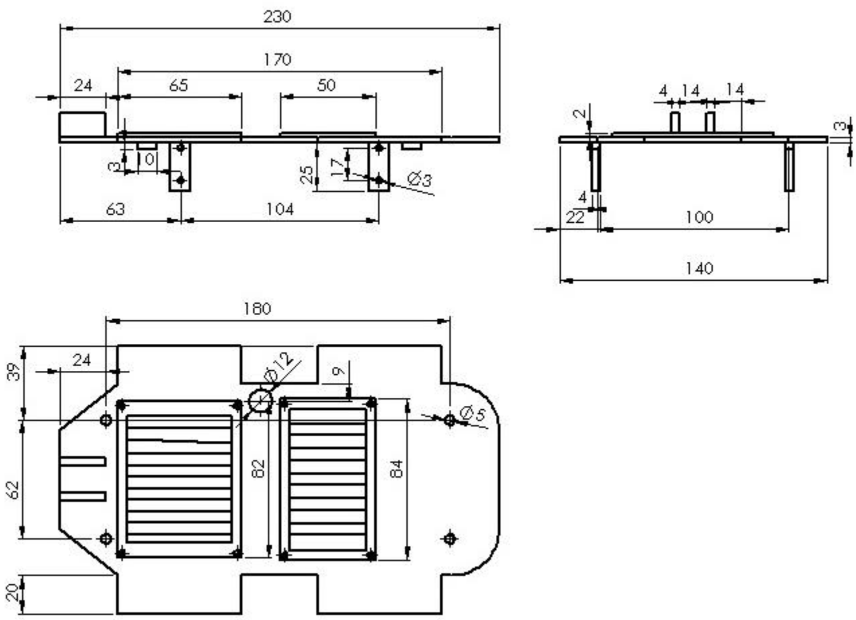


Figure 3. Chassis – improved design (Design2)

As Figure 3 demonstrates, the chassis's overall shape was changed to reduce its weight without emptying vast areas. Furthermore, the width of the chassis was set to 140 mm, and its track width was reduced to 100 mm. Finally, two areas with reduced material were designed: one measuring 82 × 65 mm to host the Arduino board and the motor shield, and another measuring 84 × 50 mm to host the battery pack.

### 2.2.1. centre of mass

The height of the centre of mass of a vehicle affects its handling; thus, before the construction of the model car, its centre of mass was calculated. The mass of each component was measured with an electronic scale, Kern FCB24K1, with a weighing range of 24 kg and readability equal to 1 g. Thereafter, the assembly of the model car was designed using Solidworks software, and the position of each component and its centre of mass was estimated computationally. Table 2 presents the mass of each component and its computationally estimated position of the centre of mass on the improved model car.

Table 2. Mass and coordinates of the centre of mass of each component of the autonomous model car

| Component | Mass (g) | Centre of mass | | |
|---|---|---|---|---|
| | | X Coordinate | Y Coordinate | Z coordinate |
| Ultrasonic module & servo motor | 24 | 70.0 | 31.2 | 214.4 |
| Battery pack | 102 | 70.0 | 9.5 | 90 |
| Board & motor shield | 60 | 70.0 | 6.0 | 167.5 |
| DC motor 1 | | 7.5 | -13.5 | 64.0 |
| DC motor 2 | 31 | 7.5 | -13.5 | 166.0 |
| DC motor 3 | | 132.5 | -13.5 | 166.0 |
| DC motor 4 | | 132.5 | -13.5 | 67.0 |
| Wheel 1 | | -19.0 | -13.5 | 36.0 |
| Wheel 2 | 41 | -16.0 | -13.5 | 36.0 |
| Wheel 3 | | 156.0 | -13.5 | 194.0 |
| Wheel 4 | | 150.0 | -13.5 | 194.0 |
| Action Camera | 199 | 70.0 | 67.6 | 17.5 |
| Chassis | 71 | 70.1 | -1.8 | 115.6 |

https://doi.org/10.55343/CogSust.150

As Table 2 illustrates, the heaviest component is the action camera, followed by the battery pack. The total mass of the model car is 744 g, and the coordinates of its centre of mass are presented in Table 3.

Table 3. Mass and coordinates of the centre of mass of the improved model car

| Mass (g) | Centre of mass | | |
|---|---|---|---|
| | X Coordinate | Y Coordinate | Z Coordinate |
| 744 | 69.9 | 15.5 | 93.1 |

### 2.3. Autonomous model car implementation

All the electronic components were mounted on the chassis and then interconnected as indicated in Figure 4 (a). Figure 4 (b) shows the complete autonomous Arduino-based improved model car (Design2).

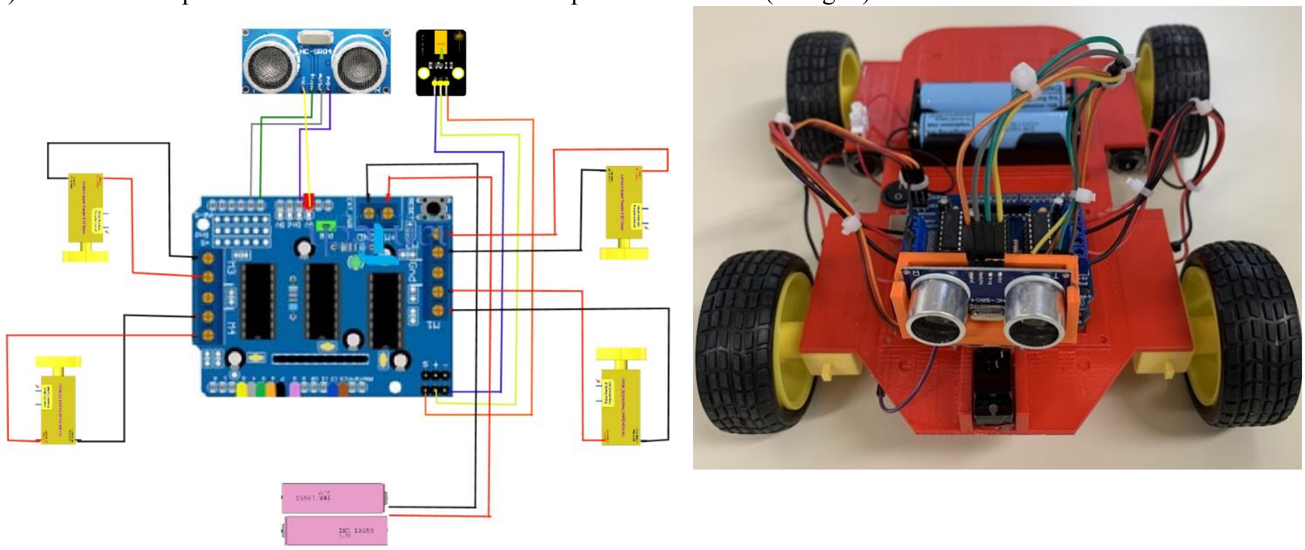

(a) (b)

Figure 4. Improved model car (Design2): (a) Circuit diagram of the electronic components and (b) Implementation of Design2

The software code must be written and uploaded to the main board for the prototype of the Arduino-based autonomous model car to become functional. The software code was developed in the Arduino IDE environment, and the libraries for the motor shield (AFMotor.h), the servomotor (Servo.h) and the ultrasonic module (NewPing.h) were added. In Figure 5, the flow chart of the algorithm is presented.

https://doi.org/10.55343/CogSust.150

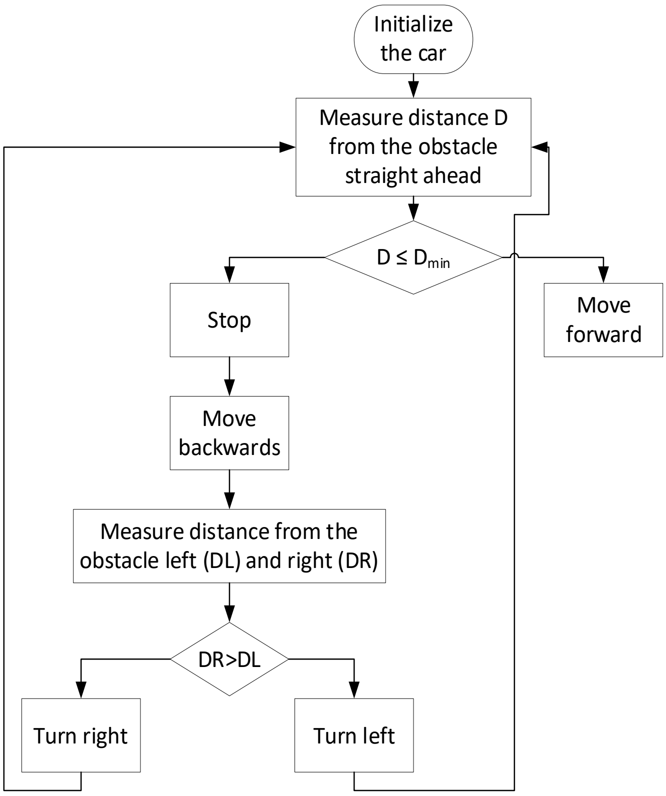

Figure 5. Flow chart of the software of MC2

During the initialisation of the model car, all four DC motors are started along with the servomotor and the ultrasonic sensor. After initiation, the DC motors move with a defined rotational speed. The servomotor starts at 0° angle. Then, the first measurement of the distance $D$ from the nearest obstacle in the forward direction is performed. If the measured distance is more than $D_{min}$, the model car moves in the forward direction. The ultrasonic sensor measures this distance repetitively. When this distance becomes less than $D_{min}$, the model car stops for 0.1 s, moves backwards for 0.2 s and stops again. Then, using the servomotor, the ultrasonic sensor turns first to the right and measures the distance from the closest obstacle in this direction ($D_R$), and then turns left to measure the corresponding distance ($D_L$) from the closest obstacle. Finally, the autonomous model car moves in the direction with the highest distance from the obstacle. If $D_R = D_L$ The model car chooses to move to the left. The cornering of the model car is achieved by altering the speeds of the inner wheel motors compared to the outer ones. In general, the software code incorporates the control of the speed and the movement of the motors, the processing of sensor data and navigation decisions.

## 3. Test of the prototype

In order to test the prototype, three different manoeuvres were designed. The autonomous model car had to move on a straight line for 3000 mm during the first manoeuvre. For the second manoeuvre, the model car navigated in a straight lane with a width of 500 mm and a length of 3000 mm, defined using discrete obstacles of height 500 mm at distances of 200 mm. For the final manoeuvre, the model car had to navigate in a square free space of 2000 × 2000 mm, bounded by discrete obstacles of a height of 500 mm. In Figure 6, the setups for all three manoeuvres are presented.

https://doi.org/10.55343/CogSust.150

(a)

(b)

https://doi.org/10.55343/CogSust.150

(c)

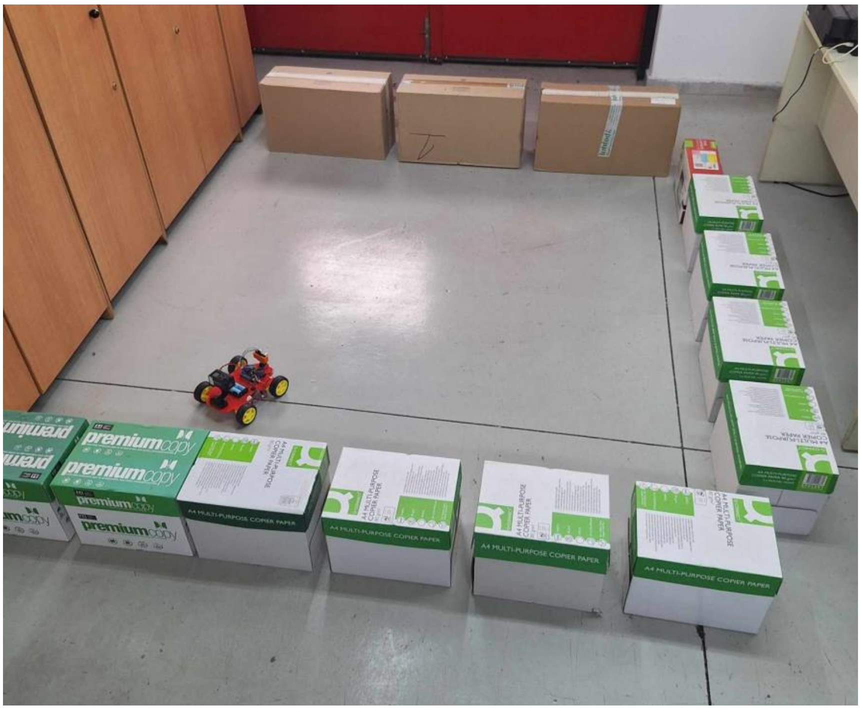


Figure 6. Manoeuvre setups (a) Test 1, (b) Test 2 and (c) Test 3

In Figures 6 (a) and (b), the model car is presented at each test's start and end. The first test was performed with three different DC motor speeds to evaluate their effect on navigation skills. The speed of the DC motors is defined through a dimensionless number that ranges from 0 to 255. In each test, the value of the dimensionless speed was set to 150, 200 and 250, respectively. In Tests 2 and 3, the value of $D_{min}$ To evaluate its effect, it was set to 250 mm, 500 mm and 1000 mm, respectively. Care was taken for the road surface to have a low friction coefficient for all test manoeuvres.

### 3.1. Results

In this section, the results of the navigation of the model car are presented for all manoeuvres.

#### 3.1.1. Test 1

Regardless of the DC motors' speed, the model car could complete Test 1. Nevertheless, it was noticed that the movement of the model car deviated from the straight line towards the left, as it is presented in Figure 7. The value of the deviation differed for different DC motor speeds.

https://doi.org/10.55343/CogSust.150

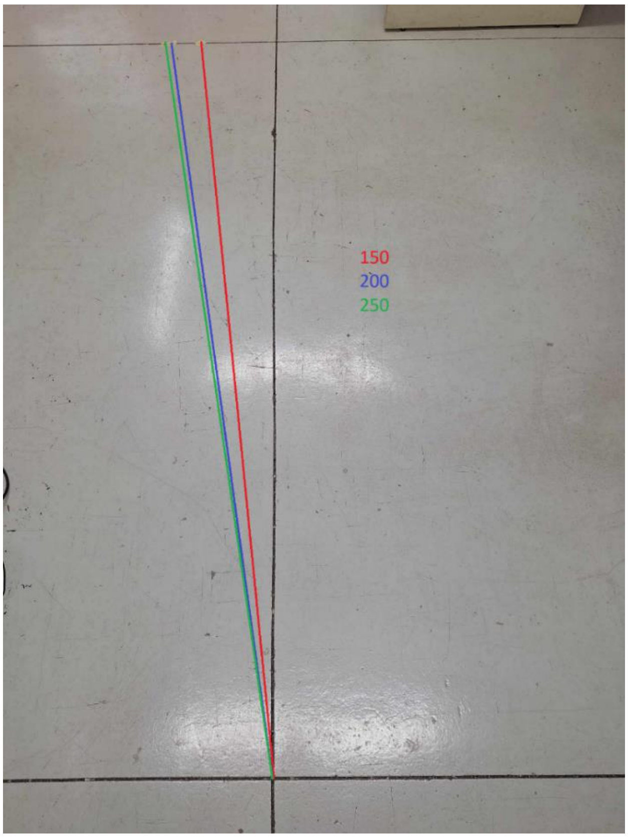

Figure 7. Model car trail for different speeds.

Table 4 presents the time needed for the model car to complete Test 1 and the measured resulting deviation.

Table 4. Results for Test 1

| **Dimensionless speed** | **Time (s)** | **Deviation (cm)** |
|---|---|---|
| 150 | 10 | 31 |
| 200 | 8 | 43 |
| 250 | 6 | 42 |

### 3.1.2. Test 2

During Test 2, the movement of the model car was restricted by a barrier. When the model car moves towards the barrier, it changes its orientation to avoid it. The influence of $D_{min}$ was evaluated along with the speed of the model car, leading to different versions of the same test manoeuvre. It was noticed that not all test manoeuvres were completed.

Table 5 presents the complete (✓) and incomplete (X) test manoeuvres.

Table 5. Test 2 was performed with different DC motor speeds and $D_{min}$

| **Dimensionless speed** | **150** | **200** | **250** |
|---|---|---|---|
| $\boldsymbol{D_{min}}$ **(mm)** | | | |
| **250** | X | X | ✓ |
| **500** | ✓ | ✓ | ✓ |
| **1000** | X | X | X |

Furthermore, in Table 6, the number of orientation changes of the model car are presented for the completed test manoeuvres, along with the total time needed to complete each test manoeuvre.

https://doi.org/10.55343/CogSust.150

Table 6. Total time and number of orientation changes for the completed manoeuvres in Test 2

| $D_{min}$ (mm) | Dimensionless Speed | Number of orientation changes | Total time to completion (s) |
|---|---|---|---|
| **250** | **250** | 1 | 9 |
| **500** | **150** | 2 | 16 |
| **500** | **200** | 4 | 22 |
| **500** | **250** | 4 | 20 |

### 3.1.3. Test 3

In Test 3, the model car was placed in the centre of a square space with dimensions of 2000 × 2000 mm and allowed to move within it. The square space was bounded by discrete obstacles as presented in Figure 6 (c). Both the DC motor speed and $D_{min}$ were altered in order to monitor the model car's dynamic behaviour. For each combination of $D_{min}$ and DC motor speed, the movement of the model car was monitored with the action camera for a total of 60 s. When $D_{min}$ was set to 250 mm, regardless of the speed of the model car, it was not using the whole space, but its movement was restricted near one of the corners of the square space. When $D_{min}$ was set to 500 mm, the model car could cover all the space in the square for the DC motor speed of 200 and 250. Finally, when $D_{min}$ was set to 1000 mm, the movement of the model car was restricted in the central area of the square space.

## 3.2. Discussion

Each test was designed to simulate a special movement condition. Therefore, Test 1 was designed to review the ability of the model car to navigate in a straight line free from obstacles. It was shown that the model car moved without changing its orientation, but it deviated from the intended direction slightly due to the quality of the wheels, the friction between the tires and the road surface, which was not smooth enough, and the position of the centre of mass of the model car. Table 7 presents the correlation between the DC motor's dimensionless speed and the model car speed for Test 1.

Table 7. Correlation between the DC motor's dimensionless speed and the model car speed

| Dimensionless speed | Calculated model car speed (m/s) |
|---|---|
| 150 | 0.30 |
| 200 | 0.38 |
| 250 | 0.50 |

Figure 8 presents the correlation between the dimensionless speed of the DC motors and the actual speed of the model car as it was calculated in Test 1.

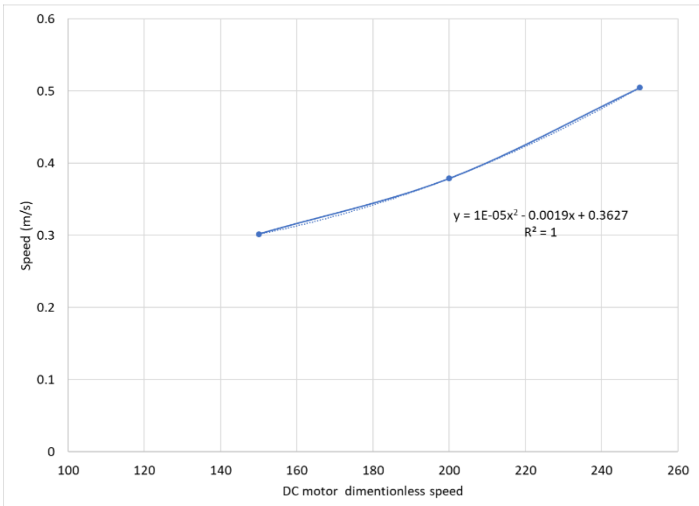


Figure 8. Correlation between the dimensionless speed of the DC motors and the speed of the model car

https://doi.org/10.55343/CogSust.150

As shown in Figure 8, the correlation between the DC motors' speed and the model car's speed is not linear. Moreover, it can be seen that increasing the DC motor speed reduces the deviation from the straight line.

Test 2 was designed to review the ability of a model car to navigate between obstacles. In this test, the influence of both the model car speed and the minimum allowed distance from an obstacle ($D_{min}$) was crucial to completing the manoeuvre as shown in Table 5. In Table 6, it was shown that as the DC motor speed increases, the number of orientation changes during the movement of the model car increases, regardless of the value of $D_{min}$. Furthermore, keeping the DC motor speed constant, the number of changes in the orientation of the model car increases with $D_{min}$.

Finally, Test 3 was designed to observe the free movement of the model car in a given space. Through this test, it was shown that the only combination of DC motor speed and $D_{min}$ that led to full space utilisation was when the dimensionless speed was set to 200 and $D_{min}$ was 500 mm. In addition, it was noticed that a low value of $D_{min}$ restricts the movement of the model car in a corner of the square space. On the other hand, if the value of $D_{min}$ is comparable to the overall dimensions of the free space, and the movement of the model car is restricted to the centre of the square space.

## 4. Chassis topology optimisation

Reviewing the performance of the autonomous model car in the test manoeuvres, the benefit of improving its response during cornering, acceleration, and braking, hence its handling characteristics, is obvious. In order to alter the handling characteristics of the model car, without adding any components, the weight of the chassis can be minimised and its dimensions can be changed. At the same time, a reduction in the weight of the chassis will reduce the total weight of the model car, lowering its environmental footprint during both construction and function phases and increasing its sustainability.

In order to ensure that the weight of the chassis can be reduced, a static finite element (FE) analysis was performed in SolidWorks Simulation Software. In Table 8, the loads applied from the electronic components, due to their weight, on the chassis are presented.

Table 8. Applied loads

| Component | Force (N) |
|---|---|
| Ultrasonic module & servo motor | 0.24 |
| Battery pack | 1.00 |
| Board & motor shield | 0.59 |
| Action Camera | 1.95 |

The areas of the attachment of the DC motors to the chassis were considered fixed supports where all the nodes' degrees of freedom were considered equal to 0. The boundary conditions of the FE model are presented in Figure 9.

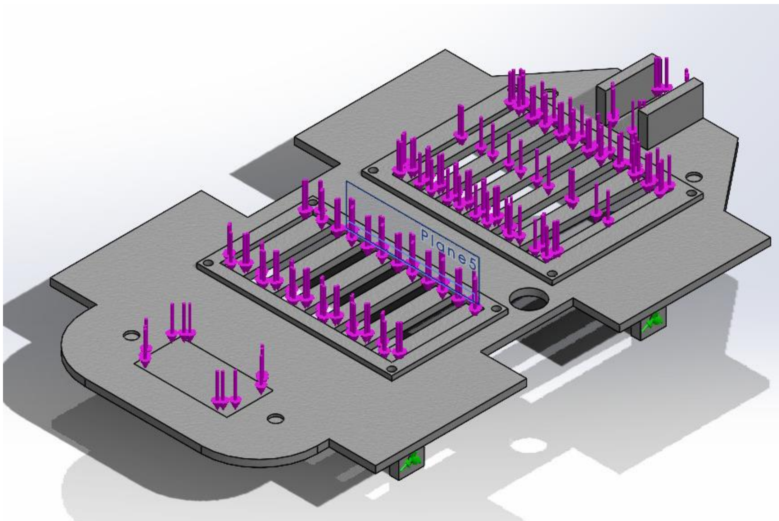

https://doi.org/10.55343/CogSust.150

Figure 9. Boundary conditions of the FE model.

In Figure 10, the mesh of the FE model is presented. The mesh was blended curvature-based, and the maximum element size was set to 5 mm, resulting in a solid mesh of 14115 FE and 28195 nodes.

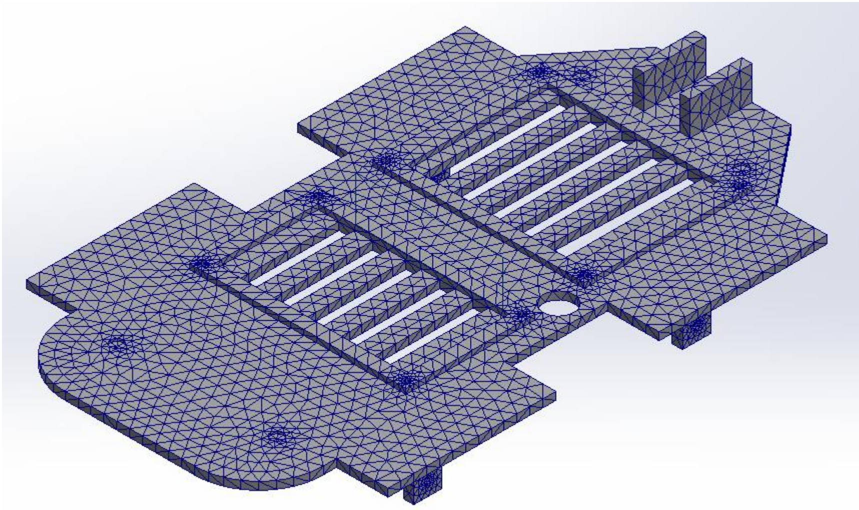

Figure 10. Mesh of the FE mode

The chassis was printed from Polylactic Acid (PLA). The physical and mechanical properties used for PLA were retrieved from the literature (Hodžić et al., 2020) for Ultimaker's PLA and are presented in Table 9.

Table 9. Physical and mechanical properties of Ultimaker's PLA (Hodžić et al., 2020)

| | |
|---|---|
| **Density (kg/m$^3$)** | 1020 |
| **Young's modulus (GPa)** | 2.9 |
| **Yield strength (MPa)** | 36.3 |
| **Tensile strength (MPa)** | 57.6 |

Figure 11 presents the Equivalent Von Mises stress (SEQV) on the chassis in an isometric and a side view.

(a)

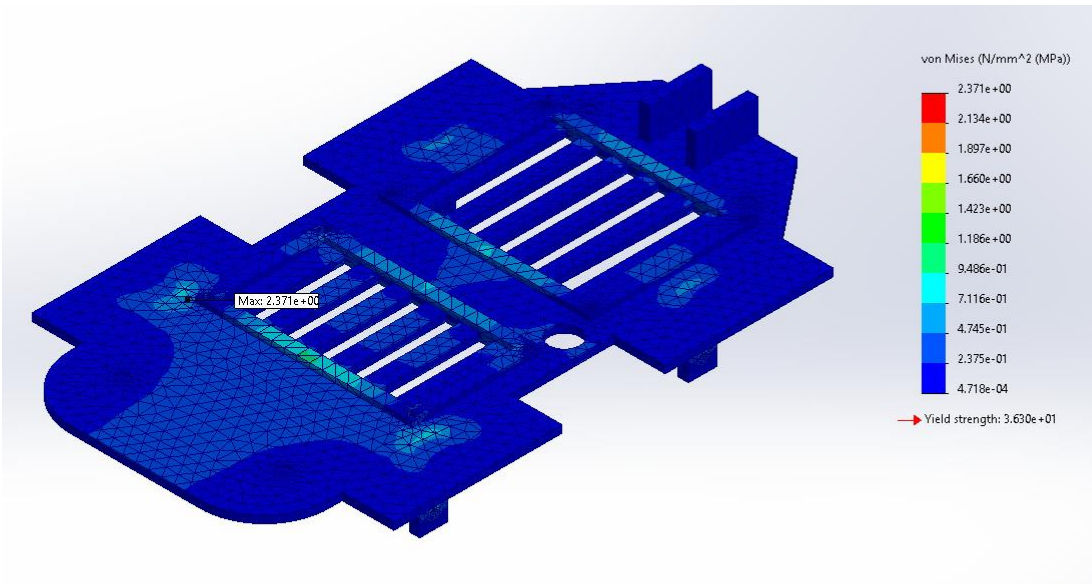

https://doi.org/10.55343/CogSust.150

(b)

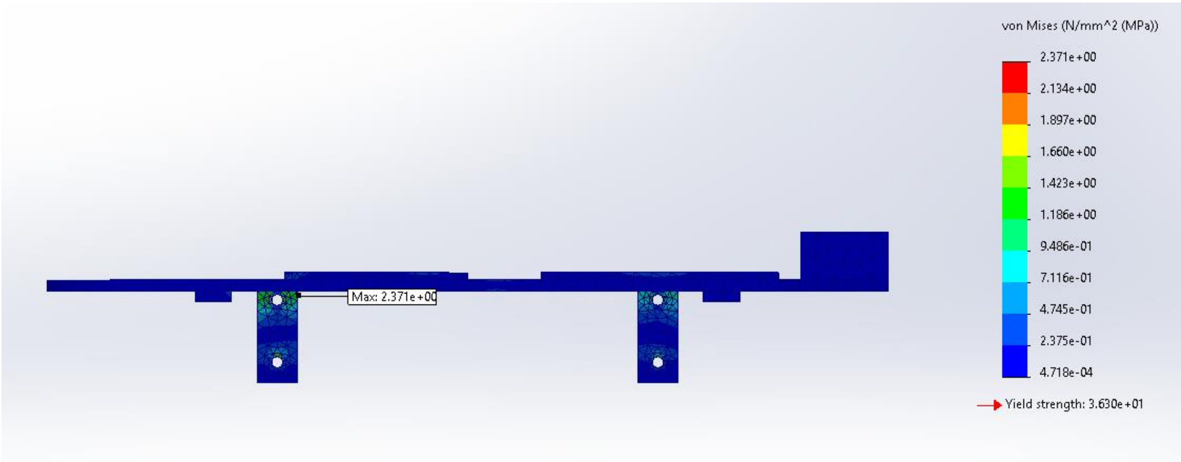


Figure 11. SEQV contour in isometric and side view

The maximum value of SEQV is located on the rear protruding structure used to support the DC motor, where it reaches 2.4 MPa. In Figure 12, the total deformation of the model is presented.

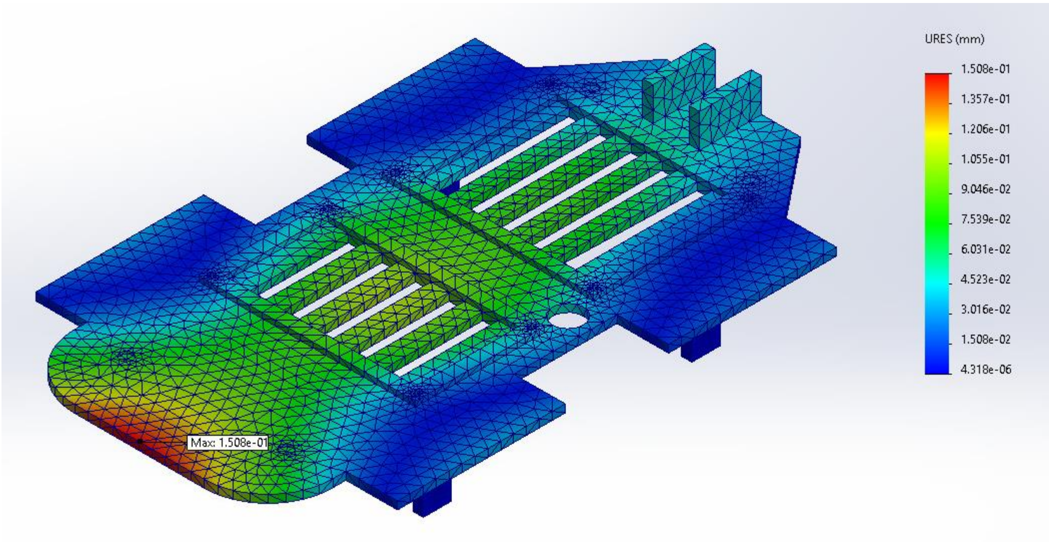


Figure 12. Total deformation contour

The maximum value of total deformation is 0.15 mm, located on the rear end of the chassis, where the action camera is mounted. The fact that the maximum value of SEQV is 6.6% of the yield strength of the material and that the displacement is less than 0.2 mm indicates that the weight of the chassis can be reduced without loss of structural integrity.

Using Design2 as the initial design of the chassis, topology optimisation was performed using the best stiffness to weight ratio as a goal, with the constraints of mass reduction by 50% and of a safety factor equal to 1.3. In Figure 13, the topology optimisation result (Design2_OPTI) is presented.

https://doi.org/10.55343/CogSust.150

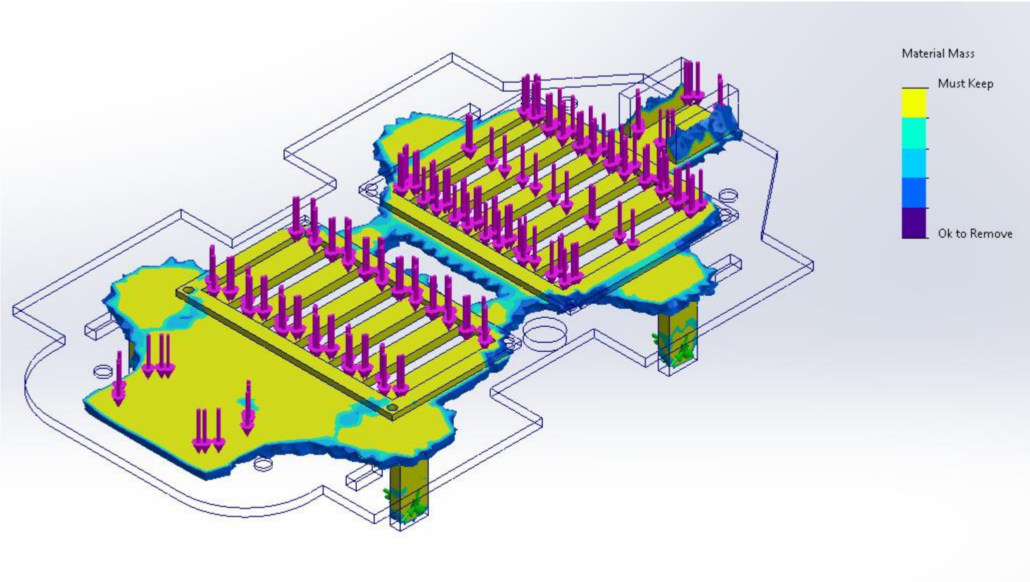


Figure 13. Results of the topology optimisation (Design2_OPTI)

As Figure 13 shows, it is obvious that material can be removed from the area in-between the structures that host the board and the battery pack, and from the rear part of the chassis. Additionally, the supporting structures of the wheels can profit from filets, but no material can be removed from those areas.

In order to further improve the dynamic behaviour of the model car, a new chassis (Design3) design was proposed based on the mean dimensions of typical vehicles. According to Zhang et al. (2022), the most common dimensions of passenger cars are presented in Table 10.

Table 10. Mean dimensions of passenger cars

| | **Length (mm)** | **Width (mm)** | **Height (mm)** |
|---|---|---|---|
| **Sedan** | 5100 | 1890 | 1560 |
| **SUV** | 4950 | 1940 | 1850 |
| **MPV** | 5150 | 1930 | 1900 |

As can be observed in Table 10, SUV vehicles are the widest, hence their dimensions were selected as a baseline for the new design of the chassis of the Arduino-based autonomous model car. Furthermore, the mean length of the wheelbase of an SUV is 2.75 m, while the mean length of the track width is 1.60 m. A typical scale for model cars that results in dimensions close to the ones of Design2 is 1:18, leading to the dimensions presented in Table 11.

Table 11. Scaled dimensions of an SUV for the Design3

| | |
|---|---|
| **Length (mm)** | 275 |
| **Width (mm)** | 108 |
| **Height (mm)** | 103 |
| **Wheelbase (mm)** | 153 |
| **Track width (mm)** | 89 |

This results in a 20% longer and 23% narrower chassis design (Design3), presented in Figure 14.

https://doi.org/10.55343/CogSust.150

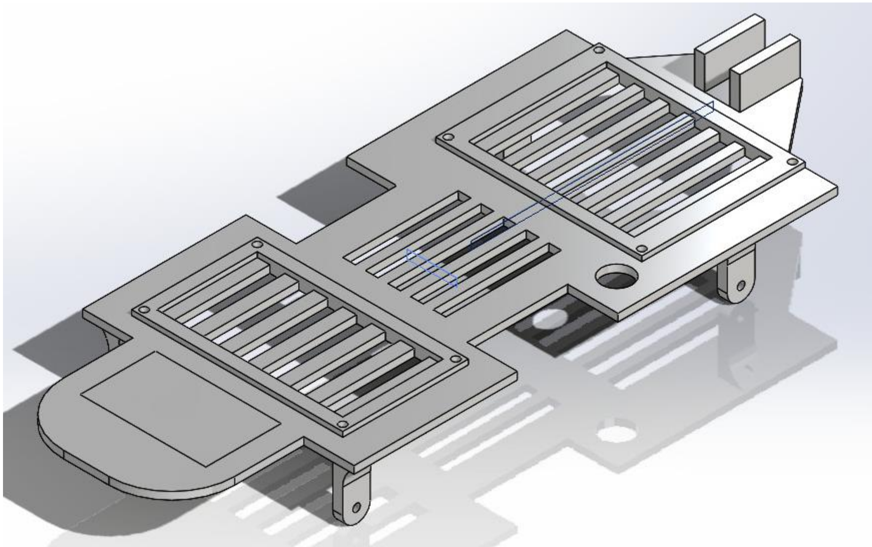

Figure 14. Chassis design based on a scaled SUV (Design3)

Figure 15 presents the topology optimisation results for the design of the chassis (Design3_OPTI). The topology optimisation was performed using the same goal, constraints, and boundary conditions as in Design2.

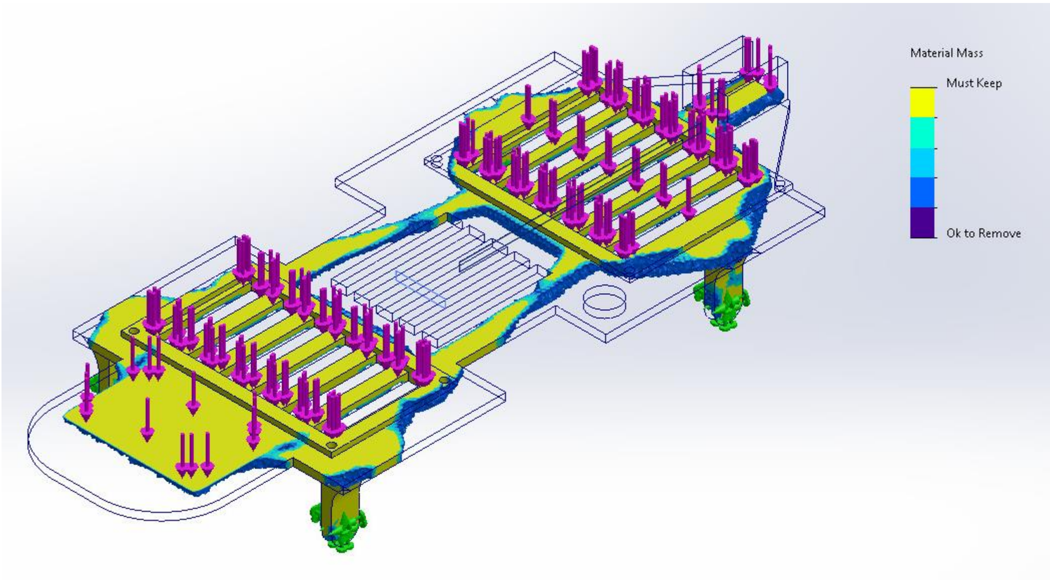


Figure 15. Results of the topology optimisation (Design3_OPTI)

In Table 12, the weight of all chassis designs is presented.

Table 12. Mass of different chassis versions

| **Chassis Versions** | **Mass (g)** |
|---|---|
| Design1 | 74 |
| Design2 | 71 |
| Design2_OPTI | 46 |
| Design3 | 69 |
| Design3_OPTI | 37 |

https://doi.org/10.55343/CogSust.150


As depicted in Table 12, the lightest design version of the chassis is Design3_OPTI, with a weight of 37 g, which is 50% lighter than the initial design (Design1).

## 5. Conclusions

In this paper, the procedure of the implementation of an optimised Arduino-based, autonomous model car is described. The selection of electronic components and the design process are presented in detail. Furthermore, the dynamic behaviour of the model car is investigated through various tests simulating different navigation conditions. Finally, alternatives for an optimised chassis design, regarding handling and sustainability, were provided using topology optimisation in Solidworks software.

Altogether, the tests of the prototype model car demonstrated that the Arduino-based autonomous model car (Design2) responded efficiently to different navigation scenarios by taking appropriate actions such as moving forward, turning left or right, and stopping to avoid collision with obstacles. Its functionality was proven more efficient for higher DC motor speed values and the minimum accepted distance from an obstacle. $D_{min}$ depending on this speed and the mean distance of the obstacles.

In the future, this Arduino-based model car can host more ultrasonic sensors to enhance its decision-making ability. Other types of sensors can be added related to its sustainability, i.e., electric power consumption. Future research directions include testing the different chassis designs, evaluating the energy consumption of the model car, integrating additional sensors, and exploring machine learning techniques for advanced decision-making. Conclusively, this Arduino-based model car can be used as a starting point to decrease true scale testing, which uses high energy resources.

## References


Ankit, V., Jigar, P., Savan, V. (2016). Obstacle avoidance robotic vehicle using ultrasonic sensor, android and Bluetooth for obstacle detection. *International Research Journal of Engineering and Technology*. 3(2), 339–348. URL: https://www.irjet.net/archives/V3/i2/IRJET-V3I257.pdf

Bao, L., Kusadokoro, M., Chitose, A., Chen, C. (2023). Development of socially sustainable transport research: A bibliometric and visualisation analysis. *Travel Behaviour and Society*. 30(2), 60–73. DOI: 10.1016/j.tbs.2022.08.012

Bhatia, A., Panchal, P. (2024). Development of an Arduino-Based Smart Robot Car for Object Detection and Navigation. *International Journal of Research in Aeronautical and Mechanical Engineering*. 12(3), 1–7. DOI: 10.5281/zenodo.10802365

Buzási, A., Csete, M. (2015). Sustainability indicators in assessing urban transport systems. *Periodica Polytechnica: Transportation Engineering*. 43(3), 138–145. DOI: 10.3311/PPtr.7825

Chen, L., Zhang, J., Wang, Y. (2018, May). Wireless car control system based on ARDUINO UNO R3. *2nd IEEE Advanced Information Management, Communicates, Electronic and Automation Control Conference (IMCEC)*. 1783–1787. DOI: 10.1109/IMCEC.2018.8469286

Ciuciu, C., Bărbuță, D., Săsăujan, S., Șipoș, E. (2017). Autonomous scale model car with ultrasonic sensors and Arduino board. *Acta Technica Napocensis*. 58(4), 6–11. DOI: https://users.utcluj.ro/~atn/papers/ATN_4_2017_2.pdf

Claes, D., Fossel, J., Broecker, B., Hennes, D., Tuyls, K. (2013). Development of an Autonomous RC-car. *Intelligent Robotics and Applications: 6th International Conference, Proceedings, Part II.* Springer, Berlin–Heidelberg. 108–120. DOI: 10.1007/978-3-642-40849-6_10

Das, N., Bhuyan, A., Sonowal, P. P., Lama, A., Boruah, N. 2024. Design and Implementation of Arduino based low cost Autonomous Car. *6th International Conference on Energy, Power and Environment (ICEPE)*. IEEE. DOI: 10.1109/ICEPE63236.2024.10668936

Eurostat (2024a). Greenhouse gas emission statistics – air emissions accounts. URL: https://ec.europa.eu/eurostat/statistics-explained/index.php?title=Archive:Greenhouse_gas_emission_statistics_-_air_emissions_accounts

Eurostat (2024b). Passenger cars in the EU. URL: https://ec.europa.eu/eurostat/statistics-explained/index.php?title=Passenger_cars_in_the_EU

Fathy, M., Ashraf, N., Ismail, O., Fouad, S., Shaheen, L., Hamdy, A. (2020). Design and implementation of self-driving car. *Procedia Computer Science*. 175, 165–172. DOI: 10.1016/j.procs.2020.07.026

Ferencz, C., Zöldy, M. (2021). Autonomous driving cycle modeling, simulation and validation on 1: 10 scale vehicle model platforms. *International Journal for Traffic and Transport Engineering (IJTTE)*. 11(4), 565–579. DOI: 10.7708/ijtte2021.11(4).06

Ferencz, C., Zöldy, M. (2022). Simulation and validation with radio-controlled (RC) autonomous vehicles in roundabout situation. *Periodica Polytechnica Transportation Engineering*. 50(3), 252–259. DOI: 10.3311/PPtr.15730

Gandotra, S., Sharma, B., Mahajan, S., Motup, T., Choudhary, T., Thakur, P. (2016). Bluetooth controlled RC car using Arduino. *Imperial Journal of Interdisciplinary Research*, 2(9), 144–147.

He, Z., Zhang, Y., Zheng, H., Zhang, Y., Yu, H., Luo, M. (2020, May). New Design of All-terrain Smart Car Based on Arduino. *IOP Conference Series: Materials Science and Engineering*. 853(1), 012046. DOI:10.1088/1757-899X/853/1/012046

Hodžić, D., Pandžić, A., Hajro, I., Tasić, P. (2020). Strength comparison of FDM 3D printed PLA made by different manufacturers. *TEM Journal*. 9(3), 966–970. DOI: 10.18421/TEM93-18

Ketter, W., Schroer, K., Valogianni, K. (2023). Information systems research for smart sustainable mobility: A framework and call for action. *Information Systems Research*. 34(3), 1045–1065. DOI: 10.1287/isre.2022.1167

Luu, D. L., Lupu, C., Chirita, D. (2019, June). Design and development of smart cars model for autonomous vehicles in a platooning. *15th International Conference on Engineering of Modern Electric Systems (EMES)*. IEEE. 21–24. DOI: 10.1109/EMES.2019.8795199

Orynycz, O. (2024). Cognitive tools for enhancing sustainability in liquid fuel and internal combustion engine development. *Cognitive Sustainability*. 3(4). DOI: 10.55343/cogsust.135

Patil, V. P., Gohatre, U., Matey, S., Jadhav, R., Kantekar A. (2022). Design and Development of Bluetooth control car based on Arduino UNO. *International Research Journal of Modernization in Engineering Technology and Science.* 4(8), 608–614. URL: https://www.irjmets.com/uploadedfiles/paper/issue_8_august_2022/29186/final/fin_irjmets1660556771.pdf

Rosen, W., Ertekin, Y., Carr, M. E. (2014, June). An autonomous Arduino-based racecar for first-year engineering technology students. *ASEE Annual Conference & Exposition*. 24–153. DOI: 10.18260/1-2--20044

SAE (2018). SAE International Recommended Practice, Taxonomy and definitions for terms related to driving automation systems for on-road motor vehicles. SAE Standard J3016_201806, Revised June 2018, Issued January 2014. DOI: 10.4271/J3016_201806

Sheeba, H., Gaur, D., Kumar Shukla, V. (2021, October). Impact of Emerging Technologies on Future Mobility in Smart Cities by 2030. *Proceedings of the 2021 9th International Conference on Reliability, Infocom Technologies and Optimisation (Trends and Future Directions)(ICRITO)*. 8–10). DOI: 10.1109/ICRITO51393.2021.9596095

Simatupang, J. W., Yosua, M. (2016). A remote controlled car using wireless technology. *Journal of Electrical And Electronics Engineering*. 1(2), 56–61. DOI: 10.33021/jeee.v1i2.192

Tang, L., Huang, W., You, J. (2019, August). The design of the intelligent car based on the Arduino UNO and Lab VIEW. *Journal of Physics Conference Series*. 1288(1):012071. DOI: 10.1088/1742-6596/1288/1/012071

Vairavan, R., Kumar, S. A., Ashiff, L. S., Jose, C. G. (2018). Obstacle avoidance robotic vehicle using ultrasonic sensor, Arduino controller. *International Research Journal of Engineering and Technology (IRJET)*. 5(2). URL: https://www.irjet.net/archives/V5/i2/IRJET-V5I2457.pdf

Vijayalakshmi, S. (2019). Robotic Car Using Arduino with Bluetooth Controller. or wirelessly controlled. *International Journal of Intelligence in Science and Engineering*. 1(1). URL: https://papers.ssrn.com/sol3/papers.cfm?abstract_id=3353197

Walke, T., Agnihotri, A., Gohate, R., Mane, S., Pande, S., Pendke, K. (2022). Miniature model of autonomous vehicle using Arduino UNO and open CV. *Ijraset Journal For Research in Applied Science and Engineering Technology*. 10(4), 3294–3305. DOI: 10.22214/ijraset.2022.42074

Yılmaz, E., Tarıyan Özyer, S. (2019). Remote and autonomous controlled robotic car based on Arduino with real time obstacle detection and avoidance. *Universal Journal of Engineering Science*. 7(1), 1–7 DOI: 10.13189/ujes.2019.070101

Zhang, J., Yang, H., Chen, Z., Yu, T., Liu, H. (2022). Probability distribution and recommended values of passenger car external dimensions in mechanical parking garage design. *Journal of Asian Architecture and Building Engineering*. 21(5), 1942–1958. DOI: 10.1080/13467581.2021.1971995

Zöldy, M., Szalmáné Csete, M. S., Kolozsi, P. P., Bordás, P., Török, Á.. (2022). Cognitive sustainability. *Cognitive Sustainability*. 1(1). DOI: 10.55343/cogsust.7